

# Enhancing Settling Performance of Precision Motion Systems by Phase-based Variable Gain Feedback Control

Luyao Dai, Xin Li, Yu Zhu, *Member, IEEE*, and Ming Zhang

**Abstract**—In this paper, phase-based variable gain feedback control (PBVGC) is utilized to improve settling performance of precision motion systems. Describing function analysis of the control strategy is presented, stability analysis is given by common quadratic Lyapunov function method and data-based tuning approach for variable gain parameter based on finite difference method is proposed. Simulation and experiment on a precision motion system both validate the phase-based variable gain feedback control algorithm and the proposed tuning approach.

**Index Terms**—phase-based variable gain feedback control, data-based tuning, precision motion systems

## I. INTRODUCTION

SETTLING performance is of paramount importance for precision motion systems, since it determines system throughput [1], [2]. Settling performance is influenced by both reference induced error and disturbance induced error. In engineering practices, settling performance is enhanced by two degree of freedom (2-DOF) control, which combines feedback and feedforward control. While feedforward control is mainly utilized for attenuation of reference induced tracking error, feedback control is mainly utilized for attenuation of external disturbance.

In engineering practices, the main components of disturbance usually distribute among low frequency range, thus the main approach for disturbance attenuation is to increase the gain of feedback controller at low frequency range. However, due to the famous water bed effect of linear control, enhancement of low frequency gain will increase sensitivity to high frequency noise and decrease stability margin [3], [4]. Therefore, nonlinear feedback control has been extensively studied in precision motion control industry [5]–[17].

In [13], [14], [16], [17], reset control, which is inspired by the classical Clegg integrator [18], [19], is proposed to improve low frequency disturbance attenuation, the output of integrator is reset under specific conditions that disturbance rejection capability can be enhanced without deteriorating overshoot and settling performance. Circle-criterion-like analysis is used to

guarantee system stability. Data-based techniques are utilized to optimize corresponding nonlinear control parameters. In [7]–[12], [15], magnitude-based variable gain control (MBVGC) is proposed to improve tracking and settling performance of precision motion systems. The nonlinear part is a piecewise affine function, where controller gain switches according to the magnitude of tracking error. Tracking error of large magnitude will lead to high controller gain and tracking error of small magnitude will lead to relatively low controller gain, thus low frequency disturbance attenuation performance can be improved while sensitivity to high frequency noise is minimized. Circle-criterion is utilized to guarantee system stability, the parameters of the piecewise affine function are still tuned by data-based method to achieve optimal performance.

MBVGC and reset control exploit circle-criterion or circle-criterion-like analysis and thus can be regarded as frequency domain techniques, to some extent. Other kinds of nonlinear feedback control strategies exist. In [20]–[22], phase-based variable gain control (PBVGC) is proposed for motion control, unlike MBVGC, the controller gain switches according to the phase of tracking error. When tracking error and its first derivative share the same sign, which means system output is going away from expected value, high gain is used, otherwise relatively low gain is used. Taking the phase of tracking error into consideration, system stability is guaranteed by Lyapunov method. Though PBVGC is a promising control strategy, further research on PBVGC is required for the following reasons:

- 1) More insight into PBVGC is required to explain the effectiveness of PBVGC.
- 2) The stability analysis in [21] is rigorous, powerful but to some extent technical, it is of practical value to develop a more simple and easy-to-use stability analysis tool.
- 3) Although data-based techniques have been widely utilized in MBVGC and reset control, there is no report on data-based techniques in PBVGC.
- 4) PBVGC has not been utilized in the precision motion control field yet.

In this paper, phase-based variable gain feedback control is studied, the main contributions of this paper can be stated as follows:

- 1) Describing function analysis of phase-based variable gain feedback control is presented, giving us more insight into the mechanism of PBVGC.

This work was supported in part by the National Key Research and Development Program of China under Grant 2018YFF01011500-04 (Corresponding author: Xin, Li).

The authors are all with the State Key Lab of Tribology, Department of Mechanical Engineering, Tsinghua University, Beijing 100084, China, and the Beijing Key Lab of Precision/Ultra-Precision Manufacture Equipment and Control, Tsinghua University, Beijing 100084, China. (e-mail: dail16@mails.tsinghua.edu.cn; lixin\_09@mail.tsinghua.edu.cn)

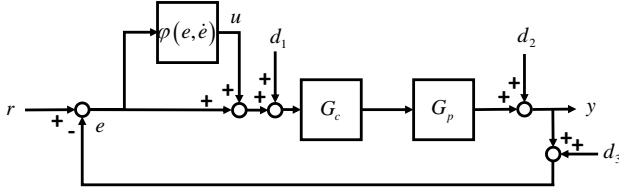


Fig. 1. Phase-based variable gain feedback control architecture.

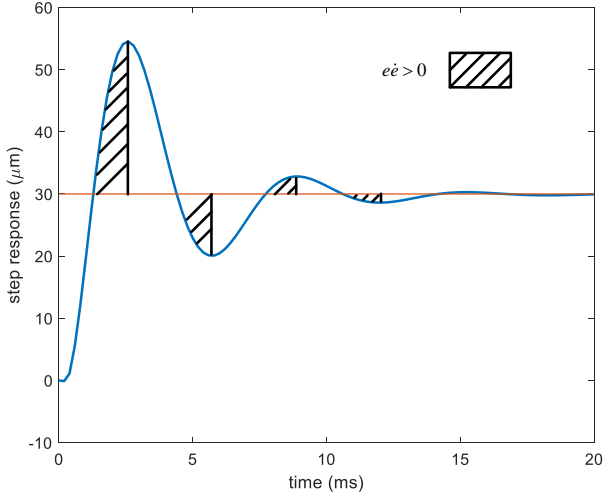


Fig. 2. Step response of a dynamic system.

2) Common quadratic Lyapunov function method is utilized to analyze the stability of PBVGC, which is easy to use and can be handily solved by available convex programming tools.

3) Data-based tuning algorithm for variable gain parameter based on finite difference method is proposed to optimize the performance of PBVGC.

4) Experiment validation on a precision linear motion system is presented.

The paper is organized as follows. Introduction is given in section I, PBVGC is introduced in detail in section II, the control architecture of PBVGC is presented first and then describing function analysis is given, which is followed by stability analysis. A data-based tuning approach for variable gain parameter based on finite difference method is presented next. Simulation results are given in section III and experiment results are given in section IV. Section V gives further discussions on corresponding topics and section VI gives conclusions of the paper.

## II. PHASE-BASED VARIABLE GAIN FEEDBACK CONTROL

PBVGC control architecture is shown in Fig. 1,  $r$  is reference trajectory,  $y$  is system output,  $e$  is tracking error,  $d_1$  is force disturbance,  $d_2$  is output disturbance,  $d_3$  is sensor noise,  $u$  is output of the variable gain part,  $G_c$  is feedback controller,  $G_p$  is plant model,  $\varphi(e, \dot{e})$  is the variable gain part

$$\varphi(e, \dot{e}) = \begin{cases} \alpha e, & e\dot{e} > 0; \\ 0, & e\dot{e} \leq 0. \end{cases} \quad (1)$$

$\alpha$  is variable gain parameter. Feedforward controller is utilized for settling performance and feedforward signal is added at the input of the plant model  $G_p$ . The diagram of feedforward controller is omitted for simplification, but note that feedforward controller does exist in the control system. The idea behind PBVGC is simple but intuitive, let us use the step response of a dynamic system to illustrate this. Fig. 2 shows the step response, the shadow area corresponds to time intervals where  $e\dot{e} > 0$ , signifying system output is going away from the expected value and thus additional gain is utilized. When  $e\dot{e} \leq 0$ , it means system output is approaching the expected value and thus no additional gain is added to the system. Such strategy can be regarded as switching control based on the phase of tracking error, see [20], [21] for more insight into the physical interpretation of PBVGC.

### A. Describing Function Analysis

In this section, describing function analysis of PBVGC is presented, which is a powerful tool to analyze the frequency domain property of the nonlinear control part, see [23], [24] for detailed discussion on describing function analysis.

Let  $e(t) = A \sin(\omega t)$  be the input of the variable gain part, then it is not hard to get that the output is

$$u(t) = \begin{cases} \alpha A \sin(\omega t), & 0 \leq t < \frac{T}{4}; \\ 0, & \frac{T}{4} \leq t < \frac{T}{2}; \\ \alpha A \sin(\omega t), & \frac{T}{2} \leq t < \frac{3T}{4}; \\ 0, & \frac{3T}{4} \leq t \leq T. \end{cases} \quad (2)$$

where  $T = \frac{2\pi}{\omega}$ . Then we can get the Fourier coefficients

$$\begin{cases} a_0 = \frac{1}{T} \int_0^T u(t) dt = 0 \\ a_1 = \frac{2}{T} \int_0^T u(t) \cos(\omega t) dt = \frac{\alpha A}{\pi} \\ b_1 = \frac{2}{T} \int_0^T u(t) \sin(\omega t) dt = \frac{\alpha A}{2} \end{cases} \quad (3)$$

Then the describing function of  $\varphi(e, \dot{e})$  is

$$\phi(j\omega) = \frac{b_1 + a_1 j}{A} = \frac{\alpha}{2} + \frac{\alpha}{\pi} j \quad (4)$$

Then we have

$$\begin{aligned} 1 + \phi(j\omega) &= 1 + \frac{\alpha}{2} + \frac{\alpha}{\pi} j \\ &= \sqrt{\left(1 + \frac{\alpha}{2}\right)^2 + \left(\frac{\alpha}{\pi}\right)^2} e^{j\Delta\phi} \end{aligned} \quad (5)$$

and

$$\Delta\phi = \arctan \frac{2\alpha}{2\pi + \alpha\pi} \quad (6)$$

After utilization of PBVGC, the open loop transfer function  $L(j\omega) = G_c G_p(j\omega)$  approximately becomes

$$\begin{aligned} L(j\omega) &\approx (1 + \phi(j\omega)) G_c G_p(j\omega) \\ &= \sqrt{\left(1 + \frac{\alpha}{2}\right)^2 + \left(\frac{\alpha}{\pi}\right)^2} e^{j\Delta\phi} G_c G_p(j\omega) \end{aligned} \quad (7)$$

The loop gain is

$$|L(j\omega)| \approx \sqrt{\left(1 + \frac{\alpha}{2}\right)^2 + \left(\frac{\alpha}{\pi}\right)^2} |G_c G_p(j\omega)| \quad (8)$$

The phase is

$$\angle(L(j\omega)) \approx \Delta\phi + \angle(G_c G_p(j\omega)) \quad (9)$$

$\angle(\cdot)$  denotes phase angle at corresponding frequency. Since  $\sqrt{\left(1 + \frac{\alpha}{2}\right)^2 + \left(\frac{\alpha}{\pi}\right)^2} > 1$ , it can provide higher gain (i.e., larger magnitude of open loop transfer function) and higher control bandwidth (the cross over frequency at 0 dB of open loop transfer function) which is good for disturbance rejection. The increase of control bandwidth may well lead to the decrease of phase margin and this can be, to some extent, compensated by  $e^{j\Delta\phi}$  which provides phase lead since  $\Delta\phi > 0$  for  $\alpha > 0$ . One of the advantages of PBVGC is that, from the perspective of describing function analysis, PBVGC is approximately equal to a complex constant rather a real constant, thus magnitude and phase of open loop transfer function can be adjusted at the same time, endowing loop shaping techniques with more flexibility.

*Remark 1* (The effect of phase lead on system stability). The dynamics of motion systems in the industry usually consists of rigid body dynamics, resonant modes and time delay, see [1], [25]–[29] for example. At low frequency range, rigid body dynamics and time delay are dominant, rigid body dynamics will introduce  $180^\circ$  phase lag and time delay will introduce additional phase lag. According to the Nyquist diagram and Nyquist stability criterion, it can be proved that the phase lag of open loop transfer function at 0 dB must be less than  $180^\circ$  to guarantee stability (i.e., the phase margin must be positive), therefore phase lead is required. Traditional linear feedback controllers, such as PID and lead-lag controller (a PID controller is in fact a special kind of lead-lag controller), provide phase lead by the lead part (i.e., the lead part of a lead-lag controller, the derivative part of a PID controller). A larger phase lead provided by the feedback controller will lead to a larger phase margin which is good for the stability of the system.

## B. Stability

As mentioned before, phase-based variable gain control is switching control based on the phase of tracking error in essence. The whole system keeps switching between two linear subsystems of different gains. Here, the two subsystems are

$$\begin{cases} G_1 = \frac{G_c G_p}{1 + G_c G_p} \\ G_2 = \frac{(1 + \alpha) G_c G_p}{1 + (1 + \alpha) G_c G_p} \end{cases} \quad (10)$$

According to [30], [31], stability can be guaranteed under arbitrary switching logic if the two subsystems are both stable and share the same quadratic Lyapunov function  $f(x) = x^T P x$ . In other words, in continuous time domain, if there exists a positive definite matrix  $P$  such that

$$\begin{cases} A_1^T P + P A_1 < 0 \\ A_2^T P + P A_2 < 0 \end{cases} \quad (11)$$

in discrete time domain, if there exists a positive definite matrix  $P$  such that

$$\begin{cases} A_1^T P A_1 - P < 0 \\ A_2^T P A_2 - P < 0 \end{cases} \quad (12)$$

then the switching system is stable under arbitrary switching logic.  $A_i$  is the system matrix of corresponding subsystem in state space,  $A_i$  can be attained by transferring transfer function  $G_i$  into state space form. This method is also called common quadratic Lyapunov function method. (11) and (12) are feasibility problem of linear matrix inequality (LMI) and can be easily solved by powerful convex programming tool such as CVX [32].

Note that the stability criterion here may be rather conservative, the conservativeness mainly originates from the following reason: (11) and (12) guarantee stability under arbitrary switching logic while switching logic of PBVGC is based on the phase of tracking error, which is a subset of arbitrary switching.

*Remark 2.* Other stability analysis techniques for PBVGC exist, see [21]. The work in [21] takes the phase of tracking error into consideration and is less conservative but much more sophisticated. Though common quadratic Lyapunov function method is more conservative, due to its simplicity, it is still a widely utilized technique in practice [31]. On the whole, both the common quadratic Lyapunov function method and the work in [21] have respective advantages and disadvantages, which one to use can be decided by the application at hand.

*Remark 3* (Circle-criterion). Aside from the common quadratic Lyapunov function method, circle-criterion method is another powerful tool for stability analysis of non-linear feedback control [23], [24]. In the study of MBVGC [10], [11], [15], the nonlinear part is a piecewise affine function which is sector-bounded and memory-less, circle-criterion can be utilized to analyze the finite  $\mathcal{L}_2$  gain stability of the closed-loop system [10]. However, PBVGC is a switching control system based on the phase of tracking error, the calculation of which requires the derivative of tracking error. Therefore, PBVGC is not memory-less and circle-criterion does not work in this situation. The differences between circle-criterion and common quadratic Lyapunov function method can be stated as follows:

1) Circle-criterion is a frequency domain tool which enables utilization of loop shaping techniques [11] while common quadratic Lyapunov method is a time domain tool which enables utilization of LMI.

2) Circle-criterion works for sector-bounded and memory-less systems, common quadratic Lyapunov method is usually utilized for switching systems.

## C. Data-based Tuning

Tuning of variable gain parameter  $\alpha$  is essential for phase-based variable gain control to take effect, since large  $\alpha$  may lead to instability and small  $\alpha$  may be unable to give enough performance. Furthermore,  $\alpha$  is disturbance dependent that the optimal  $\alpha$  varies with different kinds of disturbance.

Therefore, data-based techniques should be used for variable gain parameter tuning.

In this paper, we use quadratic cost function

$$J(\alpha) = \frac{1}{2} e^T e \quad (13)$$

Where  $e = (e_1 \ e_2 \ \dots \ e_M)^T$ ,  $M$  is the number of time instances chosen for tuning. Gauss-Newton algorithm is used

$$\alpha_{k+1} = \alpha_k - \gamma \left( \frac{\partial^2 J}{\partial \alpha^2} \right)^{-1} \frac{\partial J}{\partial \alpha} \quad (14)$$

$k$  denotes the number of iteration,  $\gamma$  is iteration step size. It is not hard to get that

$$\frac{\partial J}{\partial \alpha} = e^T \frac{\partial e}{\partial \alpha} \quad (15)$$

and

$$\frac{\partial^2 J}{\partial \alpha^2} = \frac{\partial^T e}{\partial \alpha} \frac{\partial e}{\partial \alpha} + e^T \frac{\partial^2 e}{\partial \alpha^2} \approx \frac{\partial^T e}{\partial \alpha} \frac{\partial e}{\partial \alpha} \quad (16)$$

The second order term  $e^T \frac{\partial^2 e}{\partial \alpha^2}$  mainly contains high frequency components and is usually much smaller than the first order term  $\frac{\partial^T e}{\partial \alpha} \frac{\partial e}{\partial \alpha}$  (see section 9.4 in [33] for example), therefore, the second order term is usually neglected in practice, see [2], [7], [14], [15], [34].

It can be seen that the key step of the iteration law is estimation of  $\frac{\partial e}{\partial \alpha}$ . In this paper, finite difference is used for estimation of  $\frac{\partial e}{\partial \alpha}$ , namely,

$$\frac{\partial e}{\partial \alpha} \approx \frac{e(\alpha + \Delta\alpha) - e(\alpha - \Delta\alpha)}{2\Delta\alpha} \quad (17)$$

$\Delta\alpha$  is small perturbation of  $\alpha$ . With (14)-(17),  $\alpha$  can be iteratively updated.

### III. SIMULATION

In this section, simulation results will be presented to validate the effectiveness of PBVGC and the proposed tuning approach.

#### A. Simulation Parameters

Non-collocated double-mass-block model is used in simulation, see Fig. 3. The transfer function of plant model (the plant model from force to displacement) is

$$G_{p0}(s) = \frac{1}{(m_1 + m_2)} \left( \frac{1}{s^2} - \frac{1}{s^2 + 2\zeta_n \omega_n s + \omega_n^2} \right) \quad (18)$$

$\omega_n$  and  $\zeta_n$  are resonant frequency and damping ratio, respectively. Model parameters are given in Table I. Time delay  $\tau = 1.3T$  is added to the plant,  $T = 200\mu s$  is sampling period. Time delay part is approximated by second order Pade approximation

$$e^{-s\tau} \approx \frac{1 - \frac{s\tau}{2} + \frac{s^2\tau^2}{12}}{1 + \frac{s\tau}{2} + \frac{s^2\tau^2}{12}} \quad (19)$$

By zero order hold sampling, we can get the equivalent model in discrete time domain

$$G_p(z) = \mathcal{Z} \left\{ \frac{1 - e^{-sT}}{s} \frac{1 - \frac{s\tau}{2} + \frac{s^2\tau^2}{12}}{1 + \frac{s\tau}{2} + \frac{s^2\tau^2}{12}} G_{p0}(s) \right\} \quad (20)$$

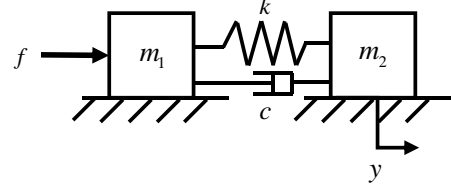


Fig. 3. Non-collocated double-mass-block model.

TABLE I  
MODEL PARAMETERS USED IN SIMULATION

$m_1$	$m_2$	$\omega_n$	$\zeta_n$
5 kg	20 kg	700 Hz	0.03

PID is used as feedback controller

$$G_c(s) = \left( k_p + k_i \frac{1}{s} + k_d \frac{s}{T_f s + 1} \right) \quad (21)$$

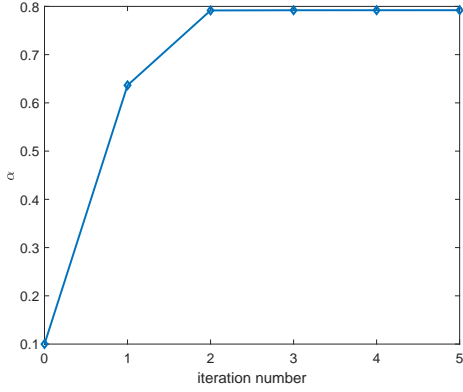
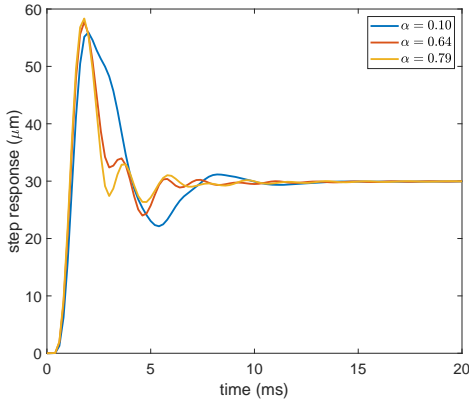
$k_p$  is proportional constant,  $k_i$  is integral constant,  $k_d$  is derivative constant,  $T_f$  is time constant of the derivative part. The control bandwidth is 180 Hz ( the crossover frequency at 0dB in the Bode diagram of open loop transfer function ). Backward difference is used to estimate  $\dot{e}$ , namely,

$$\dot{e} \approx \left( \frac{1 - z^{-1}}{T} \right) e \quad (22)$$

30  $\mu m$  step input is utilized as reference signal to validate the effectiveness of PBVGC, the reason for this choice is that, as mentioned before, PBVGC is mainly utilized for disturbance attenuation to improve settling performance, however, disturbances vary from applications to applications in practices and are thus hard to model. From a more general perspective, reference input can be regarded as a kind of external disturbance, tracking performance for reference input can also reflect the effectiveness of PBVGC. Since step response is a standard test in control engineering, we choose step input as reference signal here.

#### B. Simulation Results

Set  $\alpha_0 = 0.1$ ,  $\gamma = 1$  and  $\Delta\alpha = 0.1\alpha$ , use the data in the first 20 ms for tuning. Fig. 4 shows that  $\alpha$  converges to  $\alpha_{\text{optimal}} = 0.79$  after two iterations, Fig. 5 gives the step responses under different  $\alpha$ , it can be seen that the settling performance improves with the tuning of  $\alpha$ . Fig. 6 gives the simulation result under low gain (i.e.,  $\alpha = 0$ , the variable gain part  $\varphi(e, \dot{e})$  is not used), optimal variable gain (i.e., the variable gain part  $\varphi(e, \dot{e})$  is activated with  $\alpha = \alpha_{\text{optimal}} = 0.79$ , the feedback controller is the same with that of low gain) and high gain (i.e.,  $\alpha = 0$  and feedback controller is set as  $\tilde{G}_c = (1 + \alpha_{\text{optimal}}) G_c$ ,  $G_c$  is the feedback controller of low gain). Large vibration can be clearly observed under high gain, since stability margin is significantly reduced when high gain is taken. Comparing with low gain, the settling performance


 Fig. 4. Iteration of  $\alpha$  in simulation.

 Fig. 5. Step responses under different  $\alpha$ .

with PBVGC is largely improved, this is probably because PBVGC can, to some extent, provide both additional gain and phase lead according to the describing function analysis.

Transfer  $\frac{G_c G_p}{1+G_c G_p}$  into state space form, we can get  $A_1$ ; transfer  $\frac{(1+\alpha)G_c G_p}{1+(1+\alpha)G_c G_p}$  into state space form, we can get  $A_2$ , solve (12), if the LMIs are feasible, i.e., a  $P$  satisfying (12) can be found, then the switching system is stable under arbitrary switching. For the simulation example here, by dichotomy, it can be found the common quadratic Lyapunov function problem (12) is only feasible for  $\alpha \leq 0.65$ . However, according to simulation, the system can still work under step input with optimal value  $\alpha_{\text{optimal}} = 0.79$ . This clearly shows the conservativeness of the stability criterion given in section II-B. In engineering practices, instead of only relying on the common quadratic Lyapunov function method, simulation is extensively utilized to test system stability.

#### IV. EXPERIMENT

##### A. Experiment Platform

Experiment is carried on the precision motion pneumatic stage shown in Fig. 7. The stage is actuated by linear motor. The displacement of the stage is measured by laser interferometer with 0.15 nm resolution. The sampling period of the system is 200  $\mu$ s. Fig. 8 shows the identification result

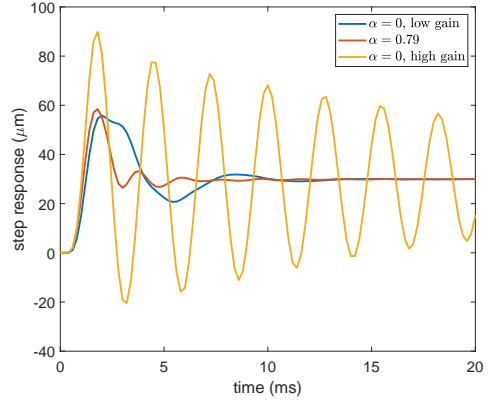


Fig. 6. Step responses under low gain, high gain and PBVGC with  $\alpha_{\text{optimal}}$ : low gain means no variable gain control is utilized, the feedback controller is  $G_c$  with 180 Hz control bandwidth;  $\alpha = 0.79$  means variable gain control with  $\alpha = \alpha_{\text{optimal}} = 0.79$  is utilized, the feedback controller is still  $G_c$ ; high gain means no variable gain control is utilized, the feedback controller is  $(1 + \alpha_{\text{optimal}}) G_c$ .

of the system. Time delay of the system is around 600  $\mu$ s. The  $-40$  dB/dec slope at low frequency range denotes the rigid body dynamics, several resonant modes exist at higher frequency range. PID is used as feedback controller, the control bandwidth is 70 Hz with  $33.5^\circ$  phase margin, the Bode and Nyquist diagram of the open loop transfer function are shown in figure Fig. 9 and Fig. 10, respectively. Instead of step response, tracking performance is focused in experiment. Fourth order trajectory shown in Fig. 11 is used as reference trajectory, detailed trajectory planning algorithm can be found in [28]. Acceleration and jerk (third derivative of reference trajectory) feedforward are used,

$$F(s) = m_a s^2 + m_j s^3 \quad (23)$$

$m_a$  is acceleration feedforward parameter,  $m_j$  is jerk feedforward parameter. The reasons for this choice of feedforward controller can be found in [26], [27]. The feedforward parameters can be tuned by the methods proposed in [26], [27]. Another important aspect has to be mentioned is that the definition of settling time varies among different fields, in precision motion control industry such as the motion control of wafer stage in lithography machine, settling time refers to the time cost it takes for tracking error to converge with an acceptable level after acceleration [1]. In experiment, we use this definition of settling time.

##### B. Experiment Results

The blue line in Fig. 12 gives the tracking performance with linear feedback and feedforward. With well-tuned feedforward controller, the capability to track reference signal can be guaranteed to a large extent, the residual tracking error can be regarded as the effect of disturbance. To further improve tracking performance, PBVGC is utilized. The initial value of variable gain parameter  $\alpha$  is set as 0.1, iteration step size  $\gamma$  is set as 1,  $\Delta\alpha$  is set as  $= 0.1\alpha$ , data during acceleration phase and the first 40 ms during constant velocity phase is used for tuning. The reason for this choice is that tracking

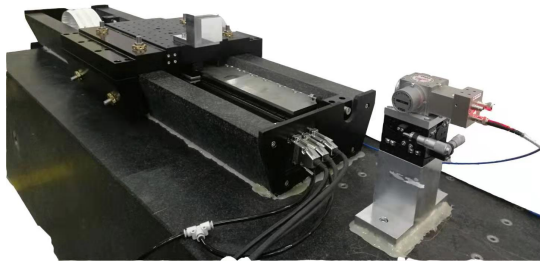


Fig. 7. Experiment platform, pneumatic stage actuated by linear motor.

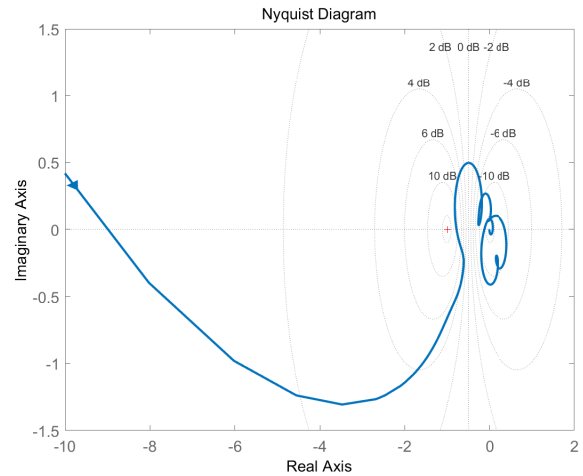


Fig. 10. Nyquist diagram of open loop transfer function.

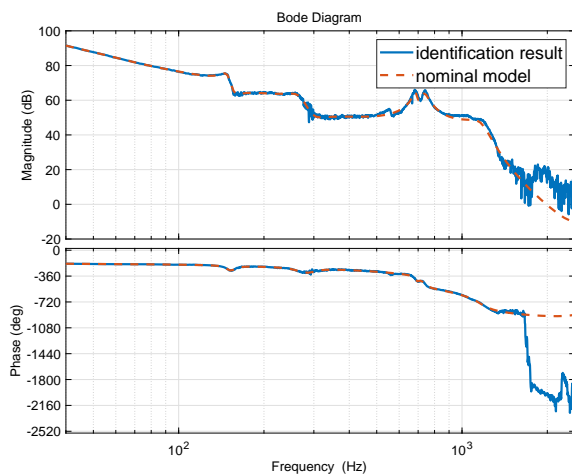


Fig. 8. System identification result.

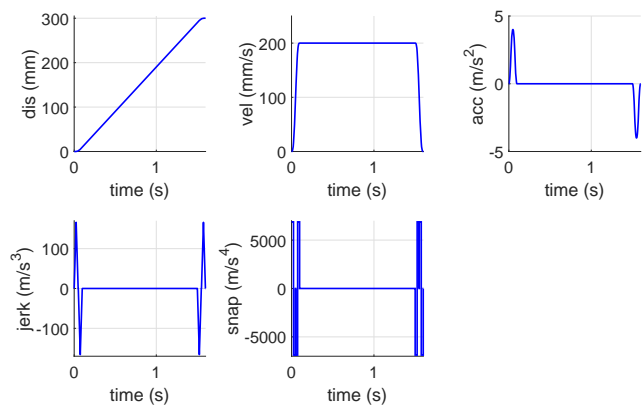


Fig. 11. Reference trajectory used in experiment, dis bound 300 mm, vel bound 200 mm/s, acc bound 4 m/s², jerk bound 166 m/s³, snap bound 6884 m/s⁴.

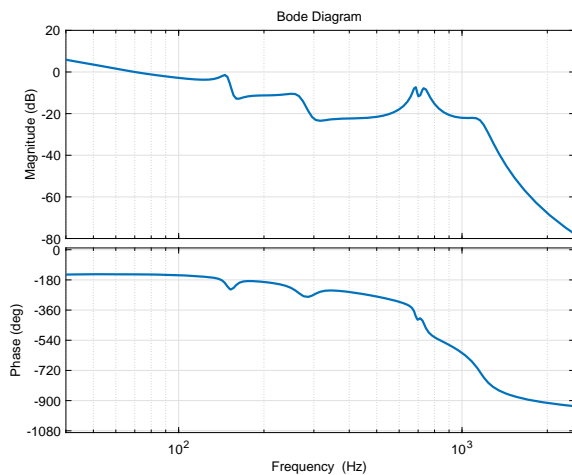


Fig. 9. Bode diagram of open loop transfer function.

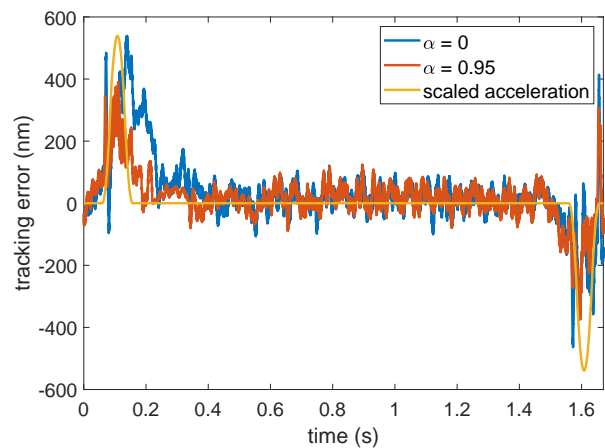


Fig. 12. Tracking performance.

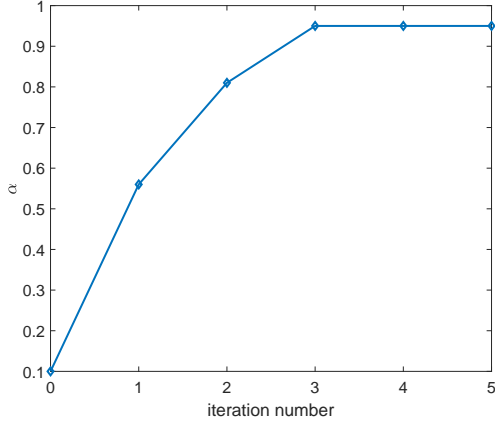
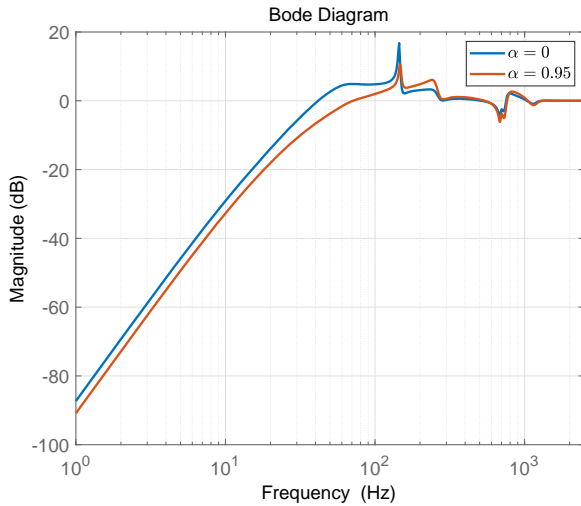

 Fig. 13. Iteration of  $\alpha$  in experiment.


Fig. 14. Bode diagram of sensitivity function.

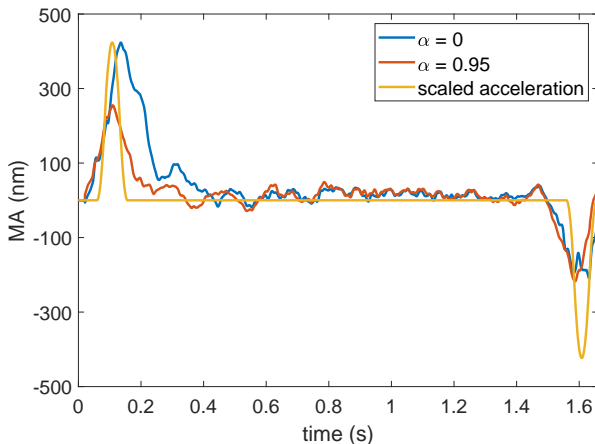


Fig. 15. Moving average plot.

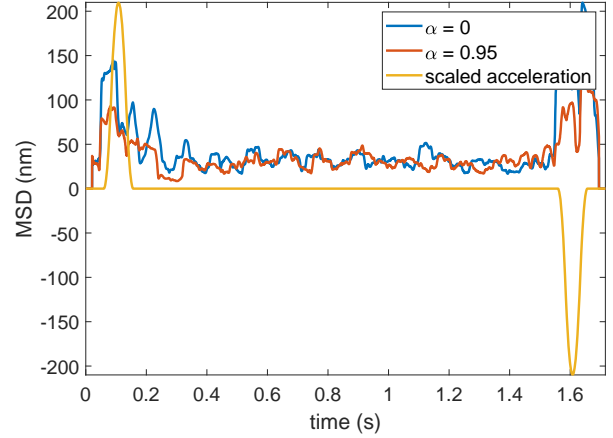


Fig. 16. Moving standard deviation plot.

error during this time interval is mainly responsible for the rise of settling time. PBVGC is only utilized during acceleration phase, deceleration phase and the first 40 ms during constant velocity phase, this is because the performance of PBVGC will be greatly impaired by noise during constant velocity phase after settling.

Fig. 13 shows the iteration of  $\alpha$ , it can be seen that  $\alpha$  converges to optimal value  $\alpha_{\text{optimal}} = 0.95$  after 3 iterations. Fig. 14 gives the Bode diagram of sensitivity function under low gain and optimal PBVGC (the Bode plot of PBVGC is attained by approximating variable gain part with describing function), it can be seen that low frequency gain is enhanced without increasing the peak of sensitivity function after use of PBVGC.

Fig. 12 gives the tracking performance of low gain and optimal PBVGC, the tracking performance of high gain where feedback controller is set as  $\tilde{G}_c = (1 + \alpha_{\text{optimal}}) G_c$  is not given, since the system becomes unstable under this gain. Moving average (MA)

$$\text{MA}(k) = \frac{1}{N} \sum_{i=k-\frac{N}{2}}^{k+\frac{N}{2}} e(i) \quad (24)$$

and moving standard deviation (MSD)

$$\text{MSD}(k) = \sqrt{\frac{1}{N} \sum_{i=k-\frac{N}{2}}^{k+\frac{N}{2}} (e(i) - \text{MA}(k))^2} \quad (25)$$

are two key performance indexes in precision motion control,  $N$  is window size. Here, we use  $N = 210$ . Fig. 15 and Fig. 16 give the MA and MSD under low gain and optimal PBVGC. It can be seen that settling performance is improved.

## V. FURTHER DISCUSSIONS

### A. The Scope of Applications and Limitations of Common Lyapunov Function Method

PBVGC in this paper just switches between two linear subsystems. In fact, common quadratic Lyapunov function method can be applied for finitely many subsystems [31],



[35], [36]. The existence of a common Lyapunov function for all subsystems is a necessary and sufficient condition for a switching system to be asymptotically stable under an arbitrary switching logic [35], [36]. If all the subsystems are linear, then the common quadratic Lyapunov function can be found by solving a set of LMIs. For example, if there are  $i$  linear discrete subsystems, then solve the feasibility problem

$$\begin{cases} A_1^T P A_1 - P < 0 \\ \vdots \\ A_i^T P A_i - P < 0 \end{cases} \quad (26)$$

if a positive definite matrix  $P$  satisfying all the LMIs can be found, then the switching system is stable under arbitrary switching logic.

As mentioned in section II-B, the main drawback of common quadratic Lyapunov function method in PBVGC is its conservativeness, since the switching logic of PBVGC is based on the phase of tracking error, which is just a subset of arbitrary switching. In other words, PBVGC may still be stable even a  $P$  cannot be found.

### B. Sensitivity to Noise

PBVGC requires  $\dot{e}$  as input, in implementation,  $\dot{e}$  is attained by real-time backward difference. Therefore  $\dot{e}$  will inevitably be influenced by noise, which will cause fast switching. That is why the PBVGC is only utilized before the settling of tracking error in the experiment, since tracking error mainly contains noise after settling.

Filtering  $\dot{e}$  may be a possible solution. However, the problem is much more complicated than it seems to be. While filtering  $\dot{e}$  can prevent fast switching, it may well attenuate the performance of PBVGC. The reason is as follows: the basic idea of PBVGC is utilizing high gain when the output of the system is going away from the expected value, which is judged by the phase of tracking error, i.e., the symbol of  $e\dot{e}$ , real-time low-pass filtering will inevitably introduce phase lag which will inevitably introduce time delay, this time delay may drastically attenuate the performance of PBVGC. To illustrate this more clearly, here, we give an simulation example, the simulation parameters are all the same with those in section III. Fig. 17 and Fig. 18 give the response with and without low-pass filtering of  $\dot{e}$ . Second order low-pass filter is used

$$G_{lp}(s) = \frac{\omega_{lp}^2}{s^2 + 2\zeta_{lp}\omega_{lp}s + \omega_{lp}^2} \quad (27)$$

$\omega_{lp} = 2\pi * 500 \text{ Hz}$ ,  $\zeta_{lp} = 0.7$ . When no filtering is used, the nonlinear part can provide additional gain when the system output is going away from the expected value (see the third subfigure in Fig. 17). When low-pass filtering is utilized, due to the time delay effect caused by low-pass filtering, the nonlinear part cannot provide additional gain at appropriate moments (see the third subfigure in Fig. 18).

### VI. CONCLUSIONS

In this paper, phase-based variable gain control in precision motion systems is studied. Describing function analysis of PBVGC is presented and data-based tuning approach for variable

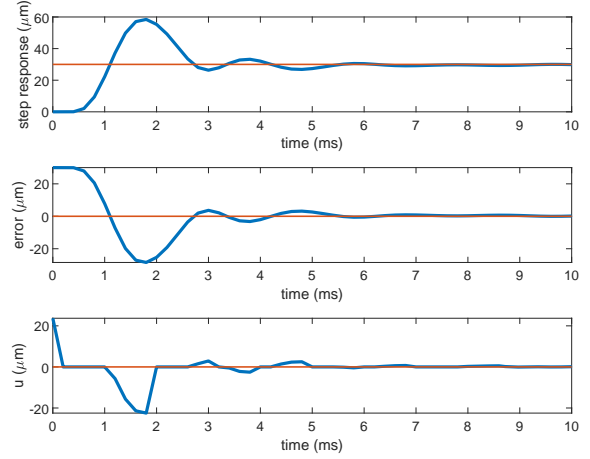


Fig. 17. The step response with  $\alpha = 0.79$ , no filtering is used,  $u$  denotes the output of the nonlinear part  $\varphi(e, \dot{e})$ .

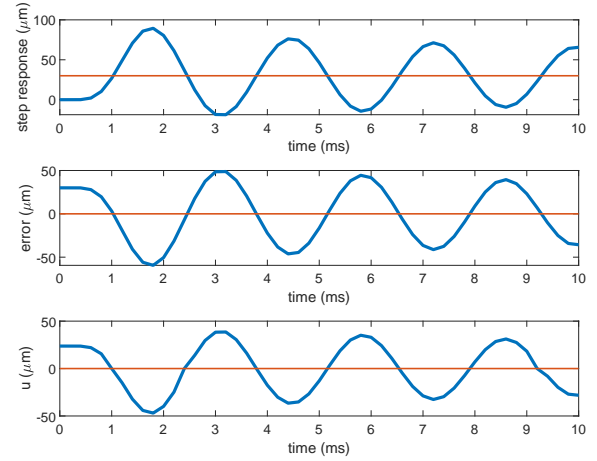


Fig. 18. The step response with  $\alpha = 0.79$ , 500 Hz second order low-pass filtering is used,  $u$  denotes the output of the nonlinear part  $\varphi(e, \dot{e})$ .

gain parameter based on finite difference method is given. Simulation and experiment on a precision motion system both validate the improvement of settling performance brought by PBVGC algorithm and the proposed tuning approach.

### ACKNOWLEDGMENT

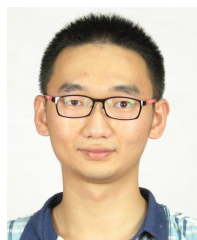
The authors thank Zhixin Su, Jiankun Zhang, Jintao Feng and Haisong Song for their crucial assistance in the experiment. The first author thanks Weicai Huang for the valuable discussion on nonlinear feedback control.

### REFERENCES

- [1] H. Butler, "Position control in lithographic equipment [applications of control]," *IEEE Control Systems*, vol. 31, DOI 10.1109/mcs.2011.941882, no. 5, pp. 28–47, Oct. 2011.
- [2] M. Heertjes, D. Hennekens, and M. Steinbuch, "MIMO feed-forward design in wafer scanners using a gradient approximation-based algorithm," *Control Engineering Practice*, vol. 18, DOI 10.1016/j.conengprac.2010.01.006, no. 5, pp. 495–506, May. 2010.



- [3] S. Skogestad and I. Postlethwaite, *Multivariable feedback control: analysis and design*, vol. 2. Wiley New York, 2007.
- [4] M. M. Seron, J. H. Braslavsky, and G. C. Goodwin, *Fundamental limitations in filtering and control*. Springer Science & Business Media, 2012.
- [5] X. Li, K. Yang, Y. Zhu, and D. Yu, "Feedforward coefficient identification and nonlinear composite feedback control with applications to 3-DOF planar motor," *Journal of Mechanical Science and Technology*, vol. 27, DOI 10.1007/s12206-013-0105-z, no. 3, pp. 895–907, Mar. 2013.
- [6] X. Li, K. Yang, Y. Zhu, and D. Yu, "Non-linear composite control with applications to 3-DOF planar motor," *Transactions of the Institute of Measurement and Control*, vol. 35, DOI 10.1177/0142331212446040, no. 3, pp. 330–341, May. 2012.
- [7] M. F. Heertjes and H. Nijmeijer, "Self-tuning of a switching controller for scanning motion systems," *Mechatronics*, vol. 22, DOI 10.1016/j.mechatronics.2011.11.001, no. 3, pp. 310–319, Apr. 2012.
- [8] B. Hunnekens, A. D. Dino, N. van de Wouw, N. van Dijk, and H. Nijmeijer, "Extremum-seeking control for the adaptive design of variable gain controllers," *IEEE Transactions on Control Systems Technology*, vol. 23, DOI 10.1109/tcst.2014.2360913, no. 3, pp. 1041–1051, May. 2015.
- [9] B. Hunnekens, N. van de Wouw, M. Heertjes, and H. Nijmeijer, "Synthesis of variable gain integral controllers for linear motion systems," *IEEE Transactions on Control Systems Technology*, vol. 23, DOI 10.1109/tcst.2014.2315657, no. 1, pp. 139–149, Jan. 2015.
- [10] M. Heertjes, F. Cremers, M. Rieck, and M. Steinbuch, "Nonlinear control of optical storage drives with improved shock performance," *Control Engineering Practice*, vol. 13, DOI 10.1016/j.conengprac.2004.11.013, no. 10, pp. 1295–1305, Oct. 2005.
- [11] M. Heertjes, X. Schuurbijs, and H. Nijmeijer, "Performance-improved design of n-PID controlled motion systems with applications to wafer stages," *IEEE Transactions on Industrial Electronics*, vol. 56, DOI 10.1109/tie.2009.2012420, no. 5, pp. 1347–1355, May. 2009.
- [12] N. van de Wouw, H. Pastink, M. Heertjes, A. Pavlov, and H. Nijmeijer, "Performance of convergence-based variable-gain control of optical storage drives," *Automatica*, vol. 44, DOI 10.1016/j.automat.2007.04.004, no. 1, pp. 15–27, Jan. 2008.
- [13] M. Heertjes, K. Gruntjens, S. van Loon, N. van de Wouw, and W. Heemels, "Experimental evaluation of reset control for improved stage performance," *IFAC-PapersOnLine*, vol. 49, DOI 10.1016/j.ifacol.2016.07.933, no. 13, pp. 93–98, 2016.
- [14] M. Heertjes, N. I. Perdiguerro, and D. Deenen, "Robust control and data-driven tuning of a hybrid integrator-gain system with applications to wafer scanners," *International Journal of Adaptive Control and Signal Processing*, vol. 33, DOI 10.1002/acs.2888, no. 2, pp. 371–387, May. 2018.
- [15] M. Heertjes, B. Hunnekens, N. van de Wouw, and H. Nijmeijer, "Learning in the synthesis of data-driven variable-gain controllers," in *2013 American Control Conference*, DOI 10.1109/acc.2013.6580889, IEEE, Jun. 2013.
- [16] D. Deenen, M. Heertjes, W. Heemels, and H. Nijmeijer, "Hybrid integrator design for enhanced tracking in motion control," in *2017 American Control Conference (ACC)*, DOI 10.23919/acc.2017.7963385, IEEE, May. 2017.
- [17] M. Heertjes, K. Gruntjens, S. van Loon, N. Kontaras, and W. Heemels, "Design of a variable gain integrator with reset," in *2015 American Control Conference (ACC)*, DOI 10.1109/acc.2015.7171052, IEEE, Jul. 2015.
- [18] J. C. Clegg, "A nonlinear integrator for servomechanisms," *Transactions of the American Institute of Electrical Engineers, Part II: Applications and Industry*, vol. 77, DOI 10.1109/taie.1958.6367399, no. 1, pp. 41–42, 1958.
- [19] L. Zaccarian, D. Nesic, and A. Teel, "First order reset elements and the clegg integrator revisited," in *Proceedings of the 2005, American Control Conference, 2005.*, DOI 10.1109/acc.2005.1470016, IEEE.
- [20] B. Armstrong, D. Neevel, and T. Kusik, "New results in NPID control: Tracking, integral control, friction compensation and experimental results," *IEEE Transactions on Control Systems Technology*, vol. 9, DOI 10.1109/87.911392, no. 2, pp. 399–406, Mar. 2001.
- [21] B. S. R. Armstrong, J. A. Gutierrez, B. A. Wade, and R. Joseph, "Stability of phase-based gain modulation with designer-chosen switch functions," *The International Journal of Robotics Research*, vol. 25, DOI 10.1177/0278364906067543, no. 8, pp. 781–796, Aug. 2006.
- [22] B. Hunnekens, N. Wouw, and D. Nešić, "Overcoming a fundamental time-domain performance limitation by nonlinear control," *Automatica*, vol. 67, DOI 10.1016/j.automat.2016.01.021, pp. 277–281, May. 2016.
- [23] H. K. Khalil, *Nonlinear systems*, vol. 3. Pearson, 2002.
- [24] J.-J. E. Slotine, W. Li *et al.*, *Applied nonlinear control*, vol. 199, no. 1. Prentice hall Englewood Cliffs, NJ, 1991.
- [25] M. Boerlage, R. Tousain, and M. Steinbuch, "Jerk derivative feedforward control for motion systems," in *American Control Conference, 2004. Proceedings of the 2004*, vol. 5, pp. 4843–4848, IEEE, 2004.
- [26] L. Dai, L. Xin, Y. Zhu, and M. Zhang, "Auto-tuning of model-based feedforward controller by feedback control signal in ultraprecision motion systems," *Mechanical Systems and Signal Processing*, vol. 142, DOI https://doi.org/10.1016/j.ymssp.2020.106764, Aug. 2020.
- [27] L. Dai, L. Xin, Y. Zhu, M. Zhang, and C. Hu, "The generation mechanism of tracking error during acceleration or deceleration phase in ultra-precision motion systems," *IEEE Transactions on Industrial Electronics*, DOI 10.1109/tie.2018.2878114, pp. 1–1, 2018.
- [28] P. Lambrechts, M. Boerlage, and M. Steinbuch, "Trajectory planning and feedforward design for electromechanical motion systems," *Control Engineering Practice*, vol. 13, DOI 10.1016/j.conengprac.2004.02.010, no. 2, pp. 145–157, Feb. 2005.
- [29] A. Preumont, *Vibration Control of Active Structures*. Springer Netherlands, 2011.
- [30] D. L. A. Morse, "Basic problems in stability and design of switched systems," *IEEE Control Systems*, vol. 19, DOI 10.1109/37.793443, no. 5, pp. 59–70, Oct. 1999.
- [31] H. Lin and P. J. Antsaklis, "Stability and stabilizability of switched linear systems: A survey of recent results," *IEEE Transactions on Automatic Control*, vol. 54, DOI 10.1109/tac.2008.2012009, no. 2, pp. 308–322, Feb. 2009.
- [32] M. Grant and S. Boyd, "CVX: Matlab software for disciplined convex programming, version 2.1," <http://cvxr.com/cvx>, Mar. 2014.
- [33] E. K. Chong and S. H. Zak, *An introduction to optimization*. John Wiley & Sons, 2004.
- [34] Y. Jiang, Y. Zhu, K. Yang, C. Hu, and D. Yu, "A data-driven iterative decoupling feedforward control strategy with application to an ultra-precision motion stage," *IEEE Transactions on Industrial Electronics*, vol. 62, DOI 10.1109/TIE.2014.2327559, no. 1, pp. 620–627, 2015.
- [35] D. Liberzon, *Switching in systems and control*. Springer Science & Business Media, 2003.
- [36] J. Zhao and D. J. Hill, "On stability,  $\mathcal{L}_2$ -gain and  $\mathcal{H}_\infty$  control for switched systems," *Automatica*, vol. 44, no. 5, pp. 1220–1232, 2008.
- [37] M. Iwasaki, K. Seki, and Y. Maeda, "High-precision motion control techniques: A promising approach to improving motion performance," *IEEE Industrial Electronics Magazine*, vol. 6, DOI 10.1109/mie.2012.2182859, no. 1, pp. 32–40, Mar. 2012.
- [38] L. Dai, X. Li, Y. Zhu, and M. Zhang, "A high performance feedforward tuning approach for ultra-precision motion control," in *Proceedings of 32nd ASPE Annual Meeting*, pp. 439–444, ASPE, 2017.
- [39] J. Daafouz, P. Riedinger, and C. Iung, "Stability analysis and control synthesis for switched systems: a switched lyapunov function approach," *IEEE Transactions on Automatic Control*, vol. 47, DOI 10.1109/tac.2002.804474, no. 11, pp. 1883–1887, Nov. 2002.
- [40] S. Pettersson and B. Lennartson, "Hybrid system stability and robustness verification using linear matrix inequalities," *International Journal of Control*, vol. 75, DOI 10.1080/0020717021000023762, no. 16-17, pp. 1335–1355, Jan. 2002.
- [41] L. Dai, L. Xin, Y. Zhu, and M. Zhang, "Quantitative tracking error analysis and feedforward compensation under different model-based feedforward controllers in different control architectures," *IEEE Transactions on Industrial Electronics*, DOI 10.1109/tie.2019.2960717, pp. 1–1, 2020.



**Luyao Dai** received B.S. degree in Mechanical Engineering from Tsinghua University, Beijing, China, in 2016. He is currently a Ph.D. candidate in Department of Mechanical Engineering, Tsinghua University. His research interest is ultra-precision motion control.



**Xin Li** received Ph.D. degree from Tsinghua University, Beijing, China, in 2013, M.S. and B.S. degrees from Dalian University of Technology, Dalian, China, in 2009 and 2006, respectively. His research interests include precision/ultra-precision motion control, robot control, especially the control and application of precision motion systems for engineering practice in industry.

He is currently an Assistant Professor in Department of Mechanical Engineering, Tsinghua University, Beijing. He has published more than

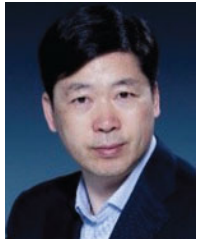
10 papers and applied for more than 10 invention patents.



**Ming Zhang** received the B.S. degree in mechanical engineering from the University of Science and Technology Beijing, Beijing, China, in 1996 and the Ph.D. degree in precision instruments from Tsinghua University, Beijing, in 2005.

He is currently an Associate Professor with the Department of Mechanical Engineering, Tsinghua University. His research interests include ultraprecision mechanical design and manufacturing, system modeling and analysis, and design of high-precision linear motors and planar motors.

sign of high-precision linear motors and planar motors.



**Yu Zhu** (M'12) received the B.S. degree in Radio Electronics from Beijing Normal University, Beijing, China, in 1983, and the M.S. degree in computer applications and the Ph.D. degree in Mechanical Design and Theory from China University of Mining and Technology, Beijing, China, in 1993 and 2001, respectively.

He is currently a Professor with the State Key Laboratory of Tribology, Department of Mechanical Engineering, Tsinghua University, Beijing, China. He has authored more than 180 technical

papers. He holds more than 50 warranted invention patents. His research interests include precision measurement and motion control, ultra-precision mechanical design and manufacturing, two-photon micro-fabrication, and electronics manufacturing technology and equipment.